was stronger than the PGK1 promoter (515 b) by 1.2-fold in terms of FVIII expression activity. Since the β-actin minimum promoter was stronger than the PGK1 promoter and was short enough to construct 5.1-kb AAV vectors carrying the BDD FVIII cDNA, we used the β-actin minimum promoter to produce AAV vectors carrying the BDD FVIII gene.

Expression of Lac Z gene by the ß-actin minimum promoter in vivo

To confirm that the β-actin minimum promoter can express a transgene in vivo, AAV vectors carrying the Lac Z gene located in the downstream of the β-actin minimum promoter (AAV1-β-actin-Lac Z, AAV8-β-actin-LacZ) were injected to wild-type mice and expression of the Lac Z gene was studied by X-gal staining. When AAV1-β-actin-Lac Z was injected to the skeletal muscles of lower extremities of wild-type mice, Lac Z gene expression was observed in muscle fibers as shown in Fig. 2A. No apparent Lac Z gene expression was observed in other organs in the AAV1-β-actin-Lac Z injected mice (not shown), suggesting that transgene expression in other organs was minimum. Lac Z gene expression of mice with intravenous injection of AAV8-β-actin-Lac Z mainly was observed in the liver as shown in Fig. 2B. Lac Z gene expression also was observed in other organs including the heart, lung, and skeletal muscles in accordance with the previous report [16]. The liver could be transduced with intravenously injected AAV8-β-actin-Lac Z almost as efficiently as intraportally injected vectors (not shown).

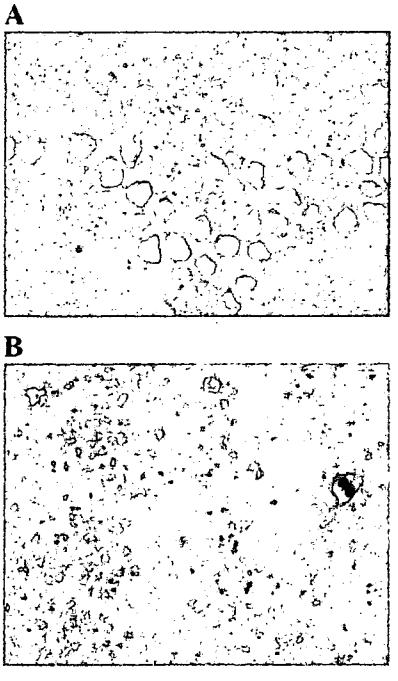

Figure 2 Expression of the Lac Z gene in mice transduced with AAV vectors carrying the Lac Z gene located downstream of the β-actin minimum promoter. X-gal staining of the skeletal muscles of mice with intramuscular injection of AAV1-β-actin-Lac Z (A) and of the liver of mice with intravenous injection of AAV8-β-actin-Lac Z (B) is shown.

Expression of FVIII by AAV vectors carrying the BDD cFVIII gene

AAV1-β-actin-FVIII vectors were injected into skeletal muscles of hemophilia A mice and AAV8-β-actin-FVIII vectors were intravenously injected into the cervical vein plexus of hemophilia A mice. FVIII clotting activities of citrated plasma drawn from mice were measured by the APTT method using FVIII-deficient human plasma.

FVIII clotting activities in mouse plasma increased on days 14 and 28 after AAV1 vector injection. The increase of FVIII clotting activities on day 28 after injection was dose-dependent. The FVIII activity levels in peripheral blood increased to $2.9 \pm 1.0\%$ in hemophilia A mice with the AAV1-β-actin-cFVIII dose of 1×10^{12} gc/body (Fig. 3), suggesting partial correction of the phenotype with AAV1-β-actin-cFVIII vectors. After these periods, FVIII activities decreased to the basal levels of mice before vector injection. FVIII antigen levels increased in parallel with levels of FVIII activity, confirming expression of cFVIII transgene in mice (not shown). Analyses for antibody against transgene products showed that neutralizing antibodies developed in 4 out of 6 tested mice by week 12 after vector injection, although the antibody titers were not high (Table 1). The RT-PCR analysis and the immunohistochemistry study suggested the presence of the transgene transcripts and products in the vector-injected muscles, suggesting that decrease of FVIII levels may be accounted for by the presence of neutralizing antibody to cFVIII.

FVIII clotting activity levels in hemophilia A mice with intravenous injection of AAV8-β-actin-cFVIII also were increased dose-dependently on day 28, achieving therapeutic FVIII levels (5–90%) in hemophilia A mice with the AAV8-β-actin-cFVIII doses of $1-3 \times 10^{11}$ gc/body and supernormal FVIII levels (180-670%) were achieved in hemophilia A mice with the AAV8-β-actin-cFVIII dose of 1×10^{12} gc/body (Fig. 4). These data on AAV8 vector-transduced FVIII expression were almost comparable with the results of the previous study using the single AAV8 vector carrying the BDD cFVIII gene [6], suggesting that β-actin minimum promoter almost

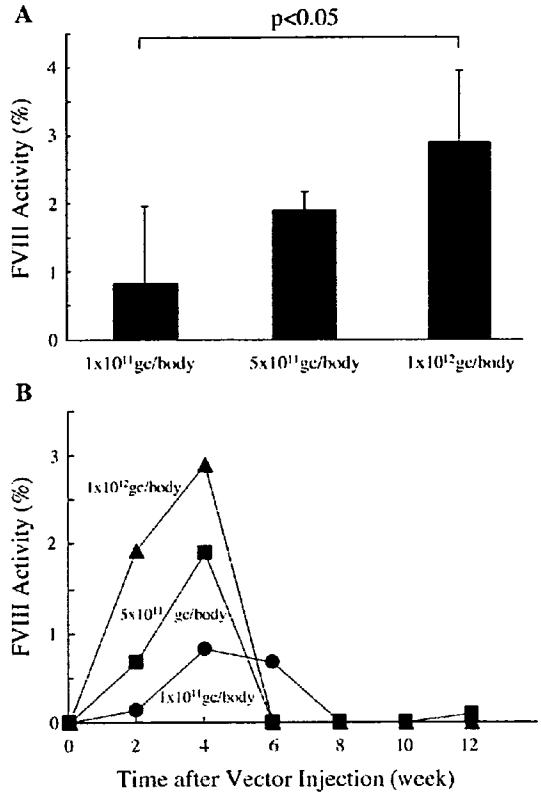

Figure 3 FVIII levels in plasma of hemophilia A mice after intramuscular injection of AAV1-β-actin-cFVIII. FVIII clotting activity levels expressed in plasma of hemophilia A mice ($n=4$) on day 28 after intramuscular injection of AAV1-β-actin-cFVIII are shown in panel A. Activity levels of cFVIII in peripheral blood of hemophilia A mice with injection of AAV1-β-actin-cFVIII (circles, 1×10^{11} gc/body: squares, 5×10^{11} gc/body: triangles, 1×10^{12} gc/body) are shown in panel B.

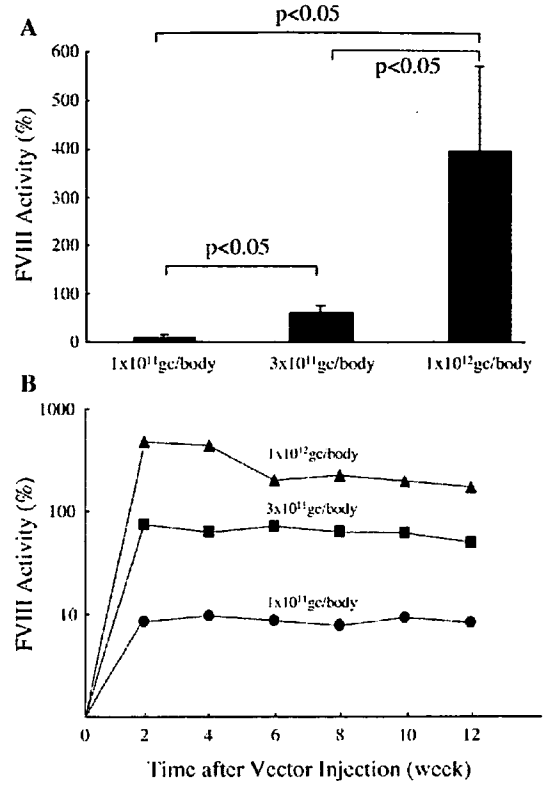

Figure 4 FVIII levels in plasma of hemophilia A mice after intravenous injection of AAV8-β-actin-cFVIII. FVIII clotting activity levels expressed in plasma of hemophilia A mice ($n=4$, each group) on day 28 after intravenous injection of AAV8-β-actin-cFVIII are shown in panel A. Activity levels of cFVIII in peripheral blood of hemophilia A mice ($n=4$, each group) with injection of AAV8-β-actin-cFVIII (circles, 1×10^{11} gc/body; squares, 3×10^{11} gc/body; triangles, 1×10^{12} gc/body) are shown in panel B.

worked as efficiently as the chimeric IGBP promoter complexes. High-level expression of FVIII in the vector-injected hemophilia A mice was sustained for more than 12 weeks. No apparent neutralizing antibody developed during the 12-week period after vector injection (Table 1). FVIII antigen levels also increased in parallel with FVIII activity levels, confirming expression of the cFVIII transgene in mice (not shown). The antigen levels of cFVIII determined by the ELISA for human FVIII were approximately 1/5 of the FVIII activity levels determined by the APTT method. Analyses for cFVIII transcripts suggested that the cFVIII gene mainly was expressed in the liver (Fig. 5) together

Table 1 Neutralizing antibodies against cFVIII developed in hemophilia A mice

	Inhibitor positive mouse	Bethesda units/mL
AAV1cFVIII	4/6 (66.7%)	9.4 ±9.5[a]
AAV8cFVIII	0/9 (0%)	Not detected

[a] Neutralizing antibodies detected by week 12 after vector injection.

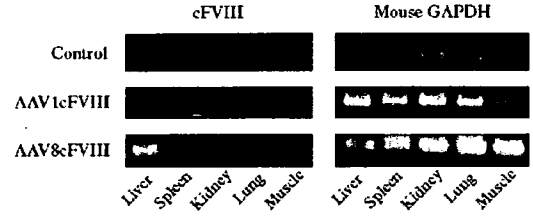

Figure 5 Analysis for cFVIII transcripts in mice. The RT-PCR analyses for the transcripts derived from the cFVIII gene (cFVIII) of RNA isolated from hemophilia A mouse organs without (control) or with intramuscular injection of AAV1-β-actin-cFVIII vectors (AAV1cFVIII) or intravenous injection of AAV8-β-actin-cFVIII vectors (AAV8cFVIII) are shown. For the control, the RT-PCR analysis for mouse GAPDH (Mouse GAPDH) of RNA isolated from hemophilia A mice with or without injection of AAV-β-actin-cFVIII vectors was performed simultaneously.

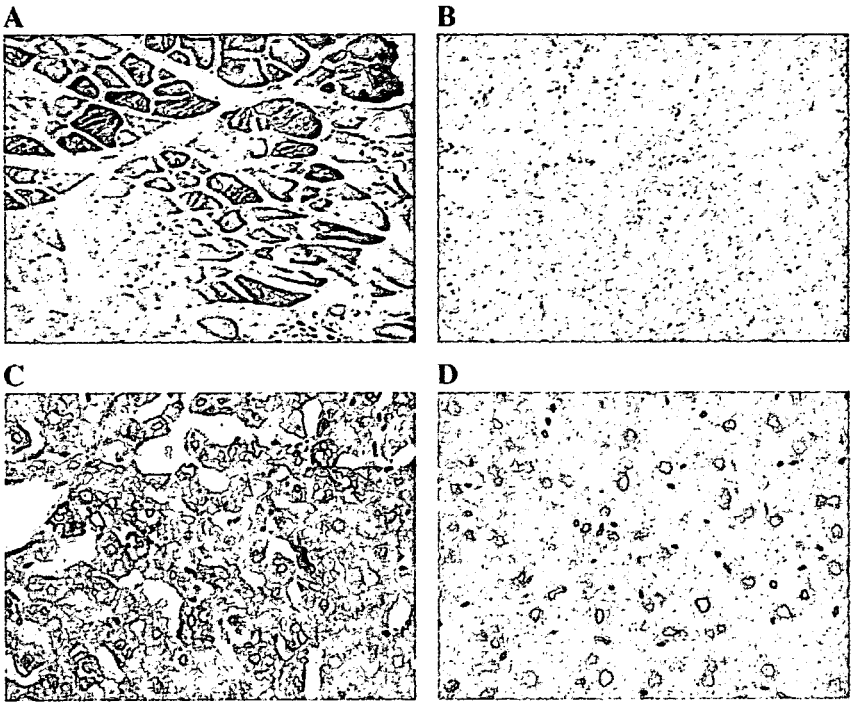

Figure 6 Immunohistochemical Analysis for cFVIII transgene products. Immunohistochemistry for cFVIII of the skeletal muscles of hemophilia A mice with intramuscular injection of AAV1-β-actin-cFVIII vectors (A) and the liver of hemophilia A mice with intravenous injection of AAV8-β-actin-cFVIII vectors (C) is shown (positive stain: brown). For the control, sections of the skeletal muscles (B) and the liver (D) obtained from hemophilia A mice without vector injection were processed simultaneously with anti-FVIII antibodies.

with the traceable expression in the heart, lung, and spleen (not shown). In accordance with the data on cFVIII transcripts, cFVIII molecules were immunohistochemically detected in the skeletal muscles of AAV1-β-actin-cFVIII injected mice and in the liver of mice with intravenous injection of AAV8-β-actin-cFVIII (Fig. 6).

Discussion

Because of the size and nature of the FVIII gene (cDNA), there were difficulties in hemophilia A gene therapy compared with gene therapy for hemophilia B. These difficulties were solved by efforts of many investigators that allowed use of a modified FVIII gene such as BDD FVIII cDNA, improved vector systems, and new strategies. Based upon these studies, a few clinical trials of hemophilia A gene therapy were conducted [17–19]. Increase of FVIII activities in the circulation and clinical improvements were observed in patients who received vector injection or transplantation of genetically modified cells. However, long-term expression of FVIII from the transgenes was not achieved in these studies. Thus, reexamination of the vector systems, the target organs for transduction, and the promoters may be required.

The recombinant AAV vectors are thought to be one of the better vectors in terms of its capability to transduce non-dividing cells and long-term transgene expression, although delivery of the FVIII gene using AAV vectors were limited by its small packaging capacity [4]. The dual AAV vector system utilizing separate AAV2 vectors independently carrying the FVIII heavy chain gene and the FVIII light chain gene could express functionally active FVIII [5]. However, there was an imbalance in the expression levels of the FVIII heavy chain and FVIII light chain, suggesting that over-expressed free FVIII light chain molecules might be more immunogenic than the native molecules. The BDD FVIII gene could be packaged in AAV2 or AAV8 vectors in the previous studies and these vectors could efficiently transduce the liver with intraportal injection of the vectors [6]. Transduction of the liver with peripheral vein injection of AAV8 vectors was as efficient as portal vein injection of vectors, although that of AAV2 vectors was not [6].

The liver would appear to be the appropriate target organ for transduction because FVIII is physiologically synthesized in this organ, so FVIII

synthesis in hepatocytes and its subsequent secretion into the circulation may be warranted. However, if any adverse reaction to the therapy occurs, removal of the liver would be an unacceptable solution. In fact minor liver dysfunction upon AAV2 vector injection into the hepatic artery was reported in clinical trials for hemophilia B gene therapy. In this respect, surgically removable organs such as skeletal muscles may well be the alternative target organs. AAV1 vector-based transduction of the skeletal muscles has beneficial characteristics of removing the transgenes. This is the first report of sufficient expression of FVIII in the skeletal muscles transduced with AAV vectors and suggests that skeletal muscle-directed FVIII expression has a potential for hemophilia A gene therapy.

Compared with synthesis and secretion of FVIII into the circulation from the liver, transport of sufficient FVIII into the circulation from the skeletal muscle fibers is not assured. Based upon our data, it is apparent that transduction of the liver with AAV8-β-actin-cFVIII is superior to transduction of skeletal muscles with AAV1-β-actin-cFVIII regarding FVIII production. The difference between FVIII levels in the peripheral blood of these vector-injected mice may be due to how the transduced cells secrete FVIII molecules into the circulation. Hepatocytes actively secrete a variety of molecules including FVIII into the circulation. Since recombinant cFVIII is in a BDD form, its expression in and secretion from hepatocytes is expected to be better than native FVIII [20], accounting for the high cFVIII expression in mice with intravenous injection of AAV8 vectors carrying the cFVIII gene though cFVIII expressing hepatocytes were not abundant. Although muscle fibers are surrounded by capillaries, transport of recombinant FVIII molecules from muscle fibers to capillaries would not be as efficient as that from hepatocytes.

In terms of the immune reaction to transgene products, muscle stem cells have been shown to function as antigen-presenting cells, suggesting that expression of the transgene by the ubiquitous promoter in the skeletal muscles might lead to development of antibodies against the transgene products if there is no immune tolerance to the transgene products [21]. This was confirmed by Wang et al. [22]. Neutralizing antibody formation was observed in 66.7% of mice with AAV1cFVIII injection even with administration of immunosuppressant, while it was not observed in mice with AAV8-β-actin cFVIII injection by week 12 after vector injection, supporting the potential advantage of AAV8 vector-based transduction of the liver over the muscle-directed transduction by AAV1 vectors.

Each vector system has advantages and disadvantages in these respects. We may need to confirm the results obtained in hemophilia mice using dogs and non-human primates that genetically are more close to humans because there may be differences in transduction efficiency of various serotypes between mice and humans [23]. Taken together, we may need to perform a comparative study using another animal models such as hemophilic dogs and non-human primates that are more genetically close to humans than mice to address these questions. Additionally, use of tissue-specific promoters to minimize neutralizing antibody formation may be a better strategy for expressing transgenes in a tissue- and organ-specific manner. These experiments will be performed in future studies.

In conclusion, our data suggested that both AAV1 and AAV8 vectors carrying the FVIII gene utilizing a minimum promoter have the potential for hemophilia A gene therapy. Our present studies have provided important insight about selecting the appropriate target for delivery of the therapeutic genes and the vector system for the hemophilia A gene therapy.

Acknowledgements

The authors are grateful to Dr. H. H. Kazazian Jr. (University of Pennsylvania, Philadelphia, PA) for FVIII-deficient mice (Hemophilia A mice), Dr. James M. Wilson (Division of Medical Genetics, Department of Medicine, University of Pennsylvania, Philadelphia, PA) for the chimeric packaging plasmid for AAV8 capsid pseudotyping, and Avigen Inc. (Alameda, CA) for the vector production system. This work is supported by Grants-in-aid for Scientific Research from the Ministry of Education and Science; Health and Labour Science Research Grants for Research from Ministry of Health, Labour and Welfare; and Grants for "High-Tech Center Research" Projects for Private Universities: matching fund subsidy from MEXT (Ministry of Education, Culture, Sports, Science, and Technology), 2002–2006.

References

[1] Hoyer LW. Hemophilia A. *N Engl J Med* 1994;330:38-47.
[2] Kay MA, High K. Gene therapy for the hemophilias. *Proc Natl Acad Sci U S A* 1999;96:9973-5.
[3] High KA. Clinical gene transfer studies for hemophilia B. *Semin Thromb Hemost* 2004;30:257-67.
[4] Lu Y. Recombinant adeno-associated virus as delivery vector for gene therapy—a review. *Stem Cells Dev* 2004; 13:133-45.

[5] Scallan CD, Liu T, Parker AE, Patarroyo-White SL, Chen H, Jiang H, et al. Phenotypic correction of a mouse model of hemophilia A using AAV2 vectors encoding the heavy and light chains of FVIII. *Blood* 2003;**102**:3919-26.

[6] Sarkar R, Tetreault R, Gao G, Wang L, Bell P, Chandler R, et al. Total correction of hemophilia A mice with canine FVIII using an AAV 8 serotype. *Blood* 2004;**103**:1253-60.

[7] Manno CS, Chew AJ, Hutchison S, Larson PJ, Herzog RW, Arruda VR, et al. AAV-mediated factor IX gene transfer to skeletal muscle in patients with severe hemophilia B. *Blood* 2003;**101**:2963-72.

[8] High KA, Manno CS, Sabatino DE, Hutchison S, Dake M, Razavi M, et al. Immune responses to AAV and to factor IX in a phase I study of AAV-mediated, liver-directed gene transfer for hemophilia B. *Blood*(suppl. 102):154a.

[9] Mochizuki S, Mizukami H, Kume A, Muramatsu S, Takeuchi K, Matsushita T, et al. Adeno-associated virus (AAV) vector-mediated liver- and muscle-directed transgene expression using various kinds of promoters and serotypes. *Gene Ther Mol Biol* 2004;**8**:9-18.

[10] Ogata K, Mimuro J, Kikuchi J, Tabata T, Ueda Y, Naito M, et al. Expression of human coagulation factor VIII in adipocytes transduced with the simian immunodeficiency virus agmTYO1-based vector for hemophilia A gene therapy. *Gene Ther* 2004;11:253-9.

[11] Kikuchi J, Mimuro J, Ogata K, Tabata T, Ueda Y, Ishiwata A, et al. Sustained transgene expression by human cord blood-derived CD34$^+$ cells transduced with simian immunodeficiency virus agmTYO1-based vectors carrying the human coagulation factor VIII gene in NOD/SCID mice. *J Gene Med* 2004;**6**:1049-60.

[12] Niwa H, Yamamura K, Miyazaki J. Efficient selection for high level expression transfectants with a novel eukaryotic vector. *Gene* 1991;**108**:193-200.

[13] Mimuro J, Muramatsu S, Hakamada Y, Mori K, Kikuchi J, Urabe M, et al. Recombinant adeno-associated virus vector-transduced vascular endothelial cells express the thrombomodulin transgene under the regulation of enhanced plasminogen activator inhibitor-1 promoter. *Gene Ther* 2001;**8**:1690-7.

[14] Bi L, Lawler AM, Antonarakis SE, High KA, Gearhart JD, Kazazian Jr HH. Targeted disruption of the mouse factor VIII gene produces a model of haemophilia A. *Nat Genet* 1995;**10**:119-21.

[15] Madoiwa S, Yamauchi T, Hakamata Y, Kobayashi E, Arai M, Sugo T, et al. Induction of immune tolerance by neonatal intravenous injection of human factor VIII in murine hemophilia A. *J Thromb Haemost* 2004;**2**:754-62.

[16] Nakai H, Fuess S, Storm TA, Muramatsu S, Nara Y, Kay MA. Unrestricted hepatocyte transduction with adeno-associated virus serotype 8 vectors in mice. *J Virol* 2005;**79**:214-24.

[17] Roth DA, Tawa Jr NE, O'Brien JM, Treco DA, Selden R.F, The Factor VIII Transkaryotic Therapy Study Group. Nonviral transfer of the gene encoding coagulation factor VIII in patients with severe hemophilia A. *N Engl J Med* 2001;**344**:1735-42.

[18] Powell JS, Ragni MV, White II GC, Lusher JM, Hillman-Wiseman C, Moon TE, et al. Phase 1 trial of FVIII gene transfer for severe hemophilia A using a retroviral construct administered by peripheral intravenous infusion. *Blood* 2003;**102**:2038-45.

[19] Chuah MK, Collen D, VandenDriessche T. Clinical gene transfer studies for hemophilia A. *Semin Thromb Hemost* 2004;**30**:249-56.

[20] Miao HZ, Kucab PF, Pipe SW. Bioengineering of coagulation factor VIII for improved secretion. *Blood* 2004;**103**:3412-9.

[21] Cao B, Bruder J, Kovesdi I, Huard J. Muscle stem cells can act as antigen-presenting cells: implication for gene therapy. *Gene Ther* 2004;11:1321-30.

[22] Wang L, Dobrzynski E, Schlachterman A, Cao O, Herzog RW. Systemic protein delivery by muscle-gene transfer is limited by a local immune response. *Blood* 2005;**105**:4226-34.

[23] Wang L, Calcedo R, Nichols TC, Bellinger DA, Dillow A, Verma IM, et al. Sustained correction of disease in naive and AAV2-pretreated hemophilia B dogs: AAV2/8-mediated, liver-directed gene therapy. *Blood* 2005;**105**:3079-86.

Available online at www.sciencedirect.com
SCIENCE DIRECT
Biochemical and Biophysical Research Communications 343 (2006) 190–197
BBRC
www.elsevier.com/locate/ybbrc

rAAV-mediated shRNA ameliorated neuropathology in Huntington disease model mouse

Yoko Machida [a], Takashi Okada [b], Masaru Kurosawa [a], Fumitaka Oyama [a], Keiya Ozawa [b], Nobuyuki Nukina [a,*]

[a] *Laboratory for Structural Neuropathology, RIKEN Brain Science Institute, 2-1 Hirosawa, Wako-shi, Saitama 351-0198, Japan*
[b] *Division of Genetic Therapeutics, Center for Molecular Medicine, Jichi Medical School, 3311-1 Yakushiji, Minami-Kawachi, Tochigi 329-0498, Japan*

Received 21 February 2006
Available online 3 March 2006

Abstract

Huntington disease (HD) is a fatal progressive neurodegenerative disorder associated with expansion of a CAG repeat in the first exon of the gene coding the protein huntingtin (htt). Although the feasibility of RNA interference (RNAi)-mediated reduction of htt expression to attenuate HD-associated symptoms is suggested, the effects of post-symptomatic RNAi treatment in the HD model mice have not yet been certified. Here we show the effects of recombinant adeno-associated virus (rAAV)-mediated delivery of RNAi into the HD model mouse striatum after the onset of disease. Neuropathological abnormalities associated with HD, such as insoluble protein accumulation and down-regulation of DARPP-32 expression, were successfully ameliorated by the RNAi transduction. Importantly, neuronal aggregates in the striatum were reduced after RNAi transduction in the animals comparing to those at the time point of RNAi transduction. These results suggest that the direct inhibition of mutant gene expression by rAVV would be promising for post-symptomatic HD therapy.

Keywords: Polyglutamine; Huntington disease; DARPP-32; Adeno-associated virus; RNAi

Huntington disease (HD) is an autosomal dominant neurodegenerative disorder, characterized by cognitive abnormalities and involuntary movements. Selective loss of brain neurons and the formation of intranuclear aggregates were observed [1]. HD is resulting from polyglutamine repeat (CAG repeat: polyQ) expansion in the protein huntingtin (htt). Expanded polyQ alters the protein conformation and then recruits many essential proteins such as transcription-regulating proteins, molecular chaperones, and ubiquitin-binding proteins [2–6]. Mutant htt also impairs the function of the ubiquitin-proteasome system [4,7] and also induces mitochondrial calcium defects [8].

For therapeutic treatment of HD, several substances, such as Congo red and trehalose, have beneficial effects to inhibit oligomerization or stabilize polyQ bearing molecules [9,10]. These approaches targeted downstream of mutant protein expression. In contrast, gene silencing by RNA interference (RNAi) targets mRNA of mutant protein in a sequence-specific manner and reduces mutant protein expression [11]. Introduction of 21-nt short interfering RNAs (siRNAs) into mammalian cells effectively inhibits endogenous genes without a non-specific viral response. Vector-based synthesis of siRNAs became available to use in various cells and tissues [12–14]. Taking advantage of this approach, gene silencing of mutant mRNA through RNAi provides a direct approach in the treatment of neurodegenerative diseases. Lentiviral vector-mediated delivery of short hairpin siRNAs (shRNAs) targeting SOD1 (superoxide dismutase 1) to the SOD1 mutant mouse resulted in the delayed onset, improvement of behavioral defects, and protection from neuronal degeneration in the spinal cord [15]. shRNAs targeting ataxin-1 were also delivered to the cerebellum by recombinant adeno-associated virus (rAAV) to improve pathological abnormalities, reduc-

* Corresponding author. Fax: +81 48 462 4796.
E-mail address: nukina@brain.riken.jp (N. Nukina).

0006-291X/$ - see front matter © 2006 Elsevier Inc. All rights reserved.
doi:10.1016/j.bbrc.2006.02.141

ing the intranuclear inclusions and restoring the cerebellar morphology [16]. In HD, many studies have suggested toxic gain-of-function by mutant htt plays a role, thus a gene silence strategy is likely a promising therapy for HD. More recently, injection of vector-based shRNA against huntingtin improved motor disturbance and neuropathological abnormalities [17,18]. Furthermore, introduction of synthesized siRNA against htt delayed disease onset with the improvement of motor disturbance, neuropathological abnormalities, and longevity in the HD model mouse [15,19]. However, these RNAi treatments were provided at the early pre-symptomatic stage of neurodegenerative disorder in each transgenic model.

Previously, a conditional model of HD using a tetracycline-regulation system showed that mice expressing a mutated htt fragment demonstrated neuronal inclusions and progressive motor dysfunction [20]. In this model, blocking expression in symptomatic mice led to the disappearance of inclusions and amelioration of the behavioral phenotype. Thus, reduction of htt expression by RNAi may attenuate HD-associated symptom progression even if treatment is carried out after the onset of symptoms. In this study, taking advantage of truncated htt-EGFP transgenic mouse in which the aggregates are visualized by EGFP fluorescence, we investigated the neuropathological changes in HD model mice by suppression of transgene with shRNAs delivered by rAAV.

Materials and methods

HD model mouse. The HD190QG transgenic mouse was used as a HD model in this study. The HD190QG transgenic mouse harbors mutant truncated N-terminal htt containing 190 CAG repeats fused with EGFP in its genome. This animal shows progressive motor abnormality, and neuropathology such as formation of aggregates in brain, and shorter viability [21]. All the experiments with mice were approved by the Animal Experiment Committee of the RIKEN Brain Science Institute.

Construction and production of rAAV. Ten candidate sequences for short hairpin RNAs targeting EGFP mRNA were ligated into a pSilencer A plasmid (Ambion, Inc., Austin, TX). Neuro2a cells were co-transfected with each shRNA in pSilencer and EGFP expression vector pEGFP-N1 (BD Biosciences Clontech, Palo Alto, CA). The effect of gene silencing was evaluated by Western blot analysis using GFP antibody (Roche Molecular Biochemicals, Indianapolis, IN) to choose an effective sequence of shRNA (shEGFP) and non-effective sequence as a control (shEGFPcontrol). The shEGFP expression cassette containing U6 promoter was obtained by PCR with primers containing a *Hind* III restriction site, forward primer: 5′-CCCAAGCTTGGGATCTTACCGCTGTTGAGA-3′ and reverse primer: 5′-CCCAAGCTTGGGCCACACTTCAAGAACTC-3′. The monomeric red fluorescence protein (mRFP) cDNA was derived from mRFP1 in pRSET$_B$ [22] and ligated into pcDNA3 (Invitrogen Corporation, Carlsbad, CA). The shEGFP expression cassette was ligated into a proviral vector plasmid bearing inverted terminal repeats derived from AAV2 or AAV5 (pAAV-LacZ or pAAV5-RNL) to create pAAV2-shEGFP or pAAV5-shEGFP. mRFP expression cassette driven by CMV promoter was also inserted into the vector plasmid to visualize transduction (Fig. 1A). rAAV-shEGFP and rAAV-shEGFPcontrol were prepared according to three-plasmid transfection protocol described previously [23,24]. The viral stock was titrated by dot-blot hybridization with plasmid standards to make a stock of 1×10^{10} genome copies/μl.

In vitro assay of shRNA effect. HEK 293 cells was transfected with the pEGFP-N1 or plasmids expressing N-terminal htt exon 1 gene containing 16, 60, and 150 CAG repeats fused with EGFP (Nhtt16QG, Nhtt60QG, and Nhtt150QG, respectively). Four hours after transfection, rAAV2-shEGFP or shEGFPcontrol was added to the culture medium at 1×10^5 genome copies/cell. The EGFP fluorescence intensity was analyzed by the Cellomics™ Array Scan®VTI System (Beckman Coulter Inc., Fullerton, CA) after 48 h of viral transduction. The relative level of GFP intensity within the RFP-positive area transduced with rAAV-shEGFP or rAAV-shEGFPcontrol was estimated.

Virus injection into the mouse brain. Virus injection was performed by using the following coordinates with respect to the bregma; 0.5 mm anterior, 2 mm lateral, 3 mm depth, 0.3 μl/min infusion rate, and 3 μl per site. An equal amount of buffer was simultaneously injected into the contralateral side of the brain. The viral injection was carried out at the age of 8 weeks or 12 weeks, and analysis was performed at the age of 24 weeks.

Detection of virus transduction and aggregates by fluorescent imager. Mouse brains were perfused and fixed overnight with 4% paraformaldehyde. Serial-cut 40-micrometer sections were analyzed with a laser-scanning imaging system (Molecular Imager FX; Bio-Rad Laboratories, Hercules, CA) with an external laser (Bio-Rad Laboratories). Sections were imaged using the 488-nm laser with the standard 530 bandpass emission filter for detection of GFP fluorescence and 532-nm laser with the standard 640 nm bandpass emission filter for detection of RFP fluorescence as described previously [21].

Immunohistochemistry and aggregate count. Serial-cut 40-micrometer free-floating sections were used for immunohistochemistry. Sections were treated with anti-RFP antibody (Clontech) followed by AlexaFluor 568-labeled anti-rabbit secondary antibody (Molecular Probes). Aggregates were counted using images of immunohistochemistry with antibodies against EGFP (Nacalai Tesque, Inc., Kyoto, Japan), htt (Chemicon International, Inc., Temecula, CA), and ubiquitin (Dako, Glostrup, Denmark) followed by detection using ABC Elite kit (Vector Laboratories, Inc., Burlingame, CA). The number of aggregates was calculated using MacSCOPE (Mitani, Tokyo, Japan) after normalizing the contrast and brightness of the digital images as described previously [10].

Filter trap assay. The striatum, cortex, and hippocampus were sampled and homogenated in 5 volumes of IMAC buffer (20 mM Hepes, pH 7.4, 140 mM potassium acetate, 1 mM magnesium acetate, and 1 mM EGTA with EDTA-free complete protease inhibitor cocktail tablets; Roche) with seven strokes using the digital homogenizer (As One, Osaka, Japan) at 1000 rpm. Homogenate containing 10 μg of protein was diluted with 0.2 ml of 2% SDS and filtered through a 0.2 μm cellulose acetate membrane (Advantec Toyo Roshi Kaisha Ltd., Tokyo Japan). Captured insoluble protein was detected by incubation with antibodies against GFP (Roche) and htt (Chemicon) followed by incubation with secondary antibodies and fluorescence substrates. Insoluble protein was quantified using LAS-1000plus/Image Gauge software (FUJIFILM, Tokyo, Japan).

In situ hybridization. For in situ hybridization, serial-cut 40-micrometer sections and non-radioactive digoxigenin-labeled cRNA probe against DARPP-32 (the dopamine- and cAMP-regulated phosphoprotein, Mr 32,000) were used as described previously [21].

Quantitative RT-PCR. Total RNA was extracted from the striatum using TRIZOL® Reagent (Invitrogen). Contaminating genomic DNA was removed with RQ1 RNase free DNase (Promega, Madison, WI) and 2 μg of total RNA was used for RT-PCR using Superscript™III First-Strand Synthesis System (Invitrogen). TaqMan PCR was performed using the TaqMan primer and probe sets as described [21]. Expression of GAPDH was estimated in each sample using the same methods for normalization.

Statistical analysis. Statistical significance was determined by Student's *t* test using StatView 5.0 (SAS Institute Inc., Cary, NC).

Results

Gene silencing by rAAV-shRNA

In vitro screening was used to identify the efficiency of mRNA ablation of shRNAs directed to EGFP and

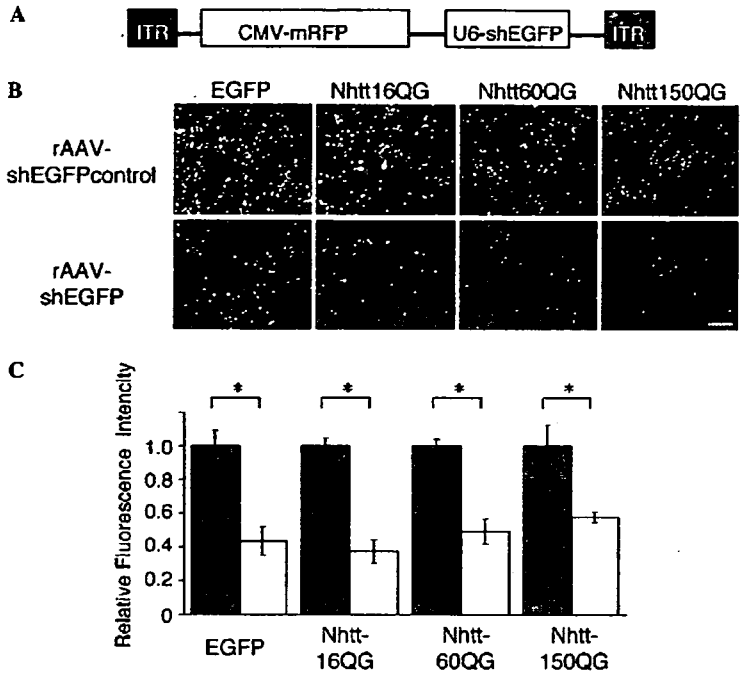

Fig. 1. rAAV-shEGFP reduced GFP expression in vitro. (A) AAV-shEGFP viral vector construct. ITR, inverted terminal repeat. CMV and U6 promoters were used for RFP and shEGFP. (B) Fluorescence photomicrographs of HEK-293 cells transfected with EGFP, Nhtt16QG, Nhtt60QG, and Nhtt150QG expression vectors and transduced with rAAV-shEGFP or rAAV-shEGFPcontrol, respectively. The photograph was taken after 48 h after viral transduction. Scale bar refers to all panels, 100 μm. (C) The relative level of GFP fluorescence intensity of rAAV-shEGFP transduced cells was compared to that of shEGFPcontrol transduced cells. The relative level of GFP fluorescence intensity of rAAV-shEGFPcontrol transduced cells (black bars); rAAV-shEGFP transduced cells (white bars). Values are given as means ± SEM ($n = 5$). $^{*}p < 0.001$.

EGFP-fused truncated htt-polyQ. EGFP-fused truncated htt-190Q is identical to the pathogenic transgene present in the HD190QG mouse [21]. The gene silencing function of 10 candidate shRNA sequences targeting EGFP was evaluated by the EGFP expression of co-transfected Neuro2A cells with shRNA and EGFP (data not shown). An shRNA targeting EGFP sequence 5′-GCAAGCTG ACCCTGAAGTTCAT-3′ (shEGFP) successfully reduced EGFP and EGFP-fused truncated htt expression significantly. Another shRNA targeting EGFP sequence 5′-GT TCATCTGCACCACCGGCTT-3′ had no gene silencing effect and was therefore used as a control (shEGFPcontrol). We next constructed an AAV-based vector (Fig. 1A). To test whether rAAV-mediated delivery of shEGFP could silence gene expression from EGFP or EGFP-fused truncated htt-polyQ, HEK293 cells were first transfected with EGFP or EGFP-fused truncated htt-polyQ expression vectors (EGFP, Nhtt16QG, Nhtt60QG, and Nhtt150QG, respectively), and subsequently transduced with rAAV2-shEGFP or rAAV2-shEGFPcontrol. shEGFP, but not shEGFPcontrol, significantly decreased GFP fluorescence intensity (Fig. 1B). The GFP intensity levels of shEGFP compared to those of shEGFPcontrol transduced cells were 0.43 ± 0.014, 0.37 ± 0.033, 0.50 ± 0.032, and 0.58 ± 0.027 (mean ± SEM, $n = 5$), in EGFP, Nhtt16QG, Nhtt60QG, and Nhtt150QG, respectively (Fig. 1C).

Expression and effect of shRNA in the mouse brain

rAAV5-shEGFP was injected into one side of the striatum and the same amount of buffer was injected into the other side of the striatum at 12 weeks old. The treated mice were sacrificed at 24 weeks old and serial-cut 40-micrometer sections were observed with laser-scanning imaging system. RFP fluorescence was expressed in the rAAV5-shEGFPinjected region and could show the infected cells (Fig. 2A). GFP fluorescence intensity was preferentially detected in the striatum, whereas the signal was decreased in the RFP-positive area. Further analysis at a higher magnification revealed that GFP fluorescent aggregates were absent in the RFP-positive neuronal cells up to three months after transduction of shEGFP in the striatum (Fig. 2B). In contrast, aggregates were abundantly observed in the contralateral side of the striatum. RFP expression was detected in the striatum as well as the cortex, lateral globus pallidus, hippocampus, and substantia nigra. However, reduction of GFP-positive aggregates was preferentially observed in the striatum, cortex, and hippocampus (data not shown).

Reduction of aggregate formation by shEGFP

Immunohistochemistry was performed using antibodies against GFP, htt, and ubiquitin. GFP and htt antibodies

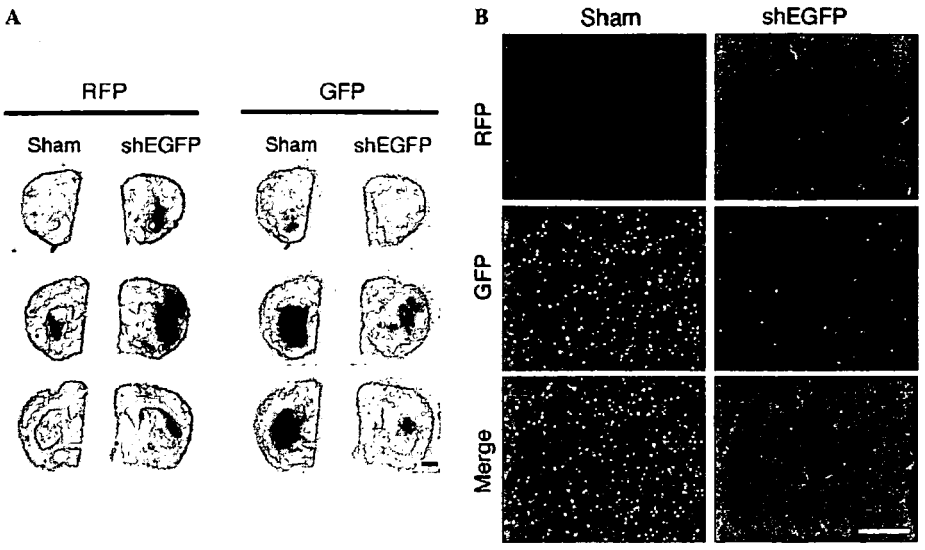

Fig. 2. rAAV-shEGFP transduction in the mouse brain decreases EGFP-positive aggregates (direct observation of EGFP fluorescence). (A) A montage of rostral-to-caudal coronal sections illustrates the extent of expression of RFP and EGFP in the brain. Three microliters of buffer was injected into striatum; sham, and rAAV-shEGFP was simultaneously injected into the contralateral side; shEGFP. Dark areas show fluorescent signal. Scale bar is 1 mm and refers to all panels. (B) EGFP fluorescence of the shEGFP-transduced striatum in high magnification. EGFP fluorescence was directly observed, while RFP was detected by anti-RFP because of the weak fluorescence after fixation. Scale bar is 20 μm and refers to all panels.

detect nuclear aggregates as well as cytoplasmic aggregates, and ubiquitin antibody detects large nuclear aggregates in HD190QG and R6/2 HD transgenic mice [10,21,25]. Reduction of aggregates is one of the indicators for the improvement of pathology in the HD mouse model [9,10,17,19]. In the HD190QG transgenic mouse, aggregate formation was first observed in the striatum at 4 weeks of age. Then, tremor, ataxia, and involuntary movements were observed at 6 weeks [21]. The shRNA was delivered to the striatum in 12 weeks old HD190QG mice to investigate the RNAi effects on disease pathology. At 24 weeks, mice brains were prepared for histological study. Immunohistochemistry was performed using antibodies against GFP, htt, and ubiquitin (Fig. 3A). The number of aggre-

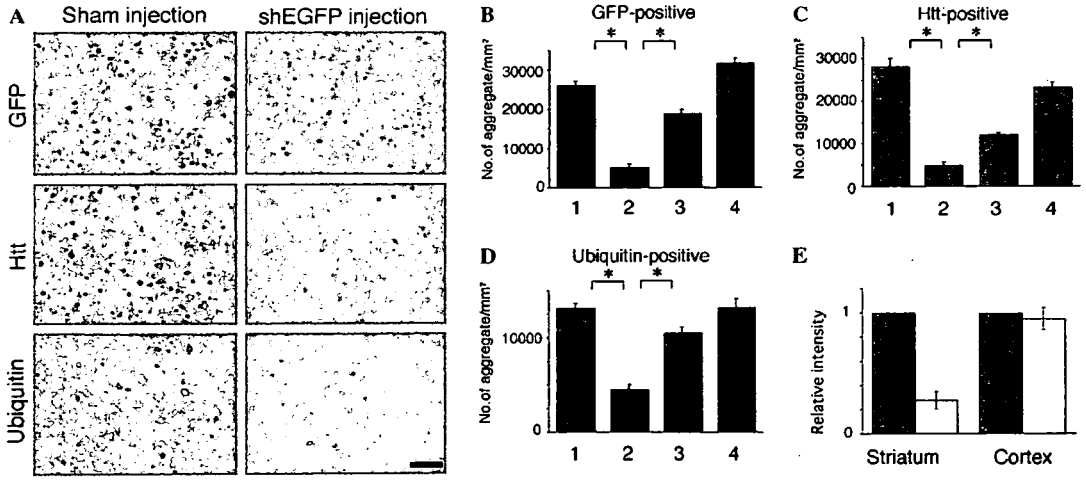

Fig. 3. shEGFP decreased antibody-positive aggregates and ameliorated aggregation pathology. (A) Representative images show GFP-, htt-, and ubiquitin-positive aggregates in the sham-injected or shEGFP-transduced striatum. Scale bar is 20 μm and refers to all panels. (B–D) Number of aggregates in the striatum is shown. rAAV-shEGFP was injected into the striatum at 12 weeks old and analyzed at 24 weeks old. The bars indicate aggregate number in the sham-injected striatum at 24 weeks old (1), shEGFP-transduced striatum at 24 weeks old (2), non-treated 12 weeks old HD190QG striatum, at the time point of shRNA transduction (3), and non-treated 24 weeks old HD190QG, as non-treatment control (4). The graphs show the number of GFP-positive aggregates (B), htt-positive aggregates (C), and ubiquitin-positive aggregates (D). Data are shown as average ± SEM (*Y* axis indicates the number of aggregates/mm^2. Sham-injected, shEGFP-transduced, and 12 weeks old control striatum; $n = 3$, 24 weeks old control striatum; $n = 4$). $^*p < 0.0001$. (E) Quantitative analysis of filter trap assay indicates relative amount of insoluble protein in the treated striatum. The relative fluorescence levels of sham-injected side (black) and shEGFP-transduced side (white) are shown as the average ± SEM ($n = 4$). $^*p < 0.0001$.

gates in the shEGFP-transduced striatum was much reduced than that in sham-injected striatum. The number of GFP-positive aggregates in shEGFP-transduced striatum was decreased to 19.4% of GFP-positive aggregates in sham injection striatum (Fig. 3B, bars 1 and 2). The number of htt-positive aggregates in shEGFP-transduced striatum was reduced to 17.7% of sham injection (Fig. 3C, bars 1 and 2), and the number of ubiquitin-positive aggregates in shEGFP-transduced striatum was reduced to 34.1% of sham injection (Fig. 3D, bars 1 and 2).

Furthermore, the number of aggregates in shEGFP-transduced striatum was significantly less than the number of aggregates formed in the striatum at the same age of shEGFP-transduction (Figs. 3B–D, bars 2 and 3). In this study, shEGFP-transduction was performed at 12 weeks old. The number of aggregate in shEGFP-transduced striatum at 24 weeks old was compared to that in 12 weeks old transgenic mice. The number of GFP-positive aggregates in shEGFP-transduced striatum was decreased to 26.8% of GFP-positive aggregates in 12 weeks old transgenic mice striatum (Fig. 3B, bars 2 and 3). The number of htt-positive aggregates in shEGFP-transduced striatum was reduced to 41.1% of 12 weeks old transgenic mice striatum (Fig. 3C, bars 2 and 3), and the number of ubiquitin-positive aggregates in shEGFP-transduced striatum was reduced to 42.9% of 12 weeks old transgenic mice striatum (Fig. 3D, bars 2 and 3). These results suggest that shEGFP was effective not only for inhibition of aggregation formation but also for clearance of aggregates that already existed in the nucleus and cytoplasm. The number of aggregates in the sham injection site was similar to that in the 24 weeks old transgenic mouse (Figs. 3B–D, bars 1 and 4). This result certifies that the injection procedure did not affect aggregation formation in the striatum. The number of aggregates was also not affected by rAAV-shEGFPcontrol transduction (data not shown).

We further investigated the effect of shEGFP on the accumulation of insoluble protein in the brain. In the HD190QG mouse brain, insoluble proteins including intra- and extra-nuclear aggregates increased in an age-dependent manner [21]. Filter trap assays revealed that insoluble protein accumulation was significantly suppressed in the shEGFP-transduced region compared to that in the sham-treated striatum, whereas it was not changed in the cortex. The reduction was 73% in the striatum and 5% in the cortex (Fig. 3E). Similar results were also obtained using htt antibody (data not shown).

Restoration of DARPP-32 expression by shRNA

To investigate the effect of shEGFP on striatal-specific transcripts, we first performed in situ hybridization using DARPP-32 probe, because DARPP-32 is known to be down-regulated in HD mouse [21,26]. We found the tendency of restored expression of DARPP-32 (Fig. 4A). Thus, we carried out the quantitative TaqMan RT-PCR analysis and confirmed that DARPP-32 and enkephalin mRNA expression was higher in the shEGFP-transduced striatum than the sham-injected side (Fig. 4B), suggesting that those gene expressions were partially restored.

Discussion

In this study, we demonstrated that neuropathological abnormalities associated with HD, such as insoluble protein accumulation and down-regulation of DARPP-32 expression, were successfully ameliorated by RNAi transduction. Following shRNA transduction, the number of neuronal aggregates in the striatum detected by ubiquitin antibody was reduced to 34.1% of that in the sham-treated striatum. Importantly, the number of aggregates in the shEGFP-transduced striatum was less than that in the striatum at the same time point of RNAi transduction.

Various treatments have shown an improvement of HD-associated abnormalities including pathological and behavioral deficits in a mouse model of HD [9,10,27–30]. Most treatments targeted downstream and possibly indirect effect of disease allele of htt, resulting in the delayed disease progression. Silencing of mutant gene expression was demonstrated using a conditional mouse model of HD [20]. Inhibition of mutant gene expression provides a direct approach to treat neurodegenerative diseases caused by toxic gain of function. RNAi is promising as a powerful tool for targeting gene knockdown. The silencing effect of synthesized siRNA injection was sustained more than 14 days in the newborn mouse brain to delay onset and prolong the life span of R6/2 [19]. In contrast, vector-based RNAi stably persisted more than 2–5 months after transduction, resulting in the improvement of motor dysfunction and neuropathological abnormalities [17,18]. AAV5 is efficient to transduce neuronal cells in the mouse brain [17,31,32], and shRNA expression by U6 promoter has been reported in mouse striatum [17]. Here we showed a drastic improvement of HD pathology in the mouse brain by rAAV5-mediated delivery of shRNA even the transduction was performed after the pathology appeared.

RNAi-mediated strategy has been performed as a pre-symptomatic treatment in the previous studies. We investigated whether RNAi treatment is functional on the pathology in the HD model after onset of disease. Gene silencing effects were observed at 2 weeks after virus injection in the symptomatic brain (data not shown), and the effect lasted for more than 3 months. Aggregate formation was effectively inhibited by shRNA transduction and the number of aggregates was decreased significantly compared with that in animals at the age of transduction. This result suggests that AAV-mediated delivery of shRNA could realize stable acquired gene knockdown in the transgenic mouse, and aggregate pathology was ameliorated as reported previously [20].

Expression of mutant htt leads to a decreased level of a subset of striatal-specific mRNAs of the HD190QG, R6/2, and R6/1 mouse [18,21,26]. DARPP-32, which is predominantly expressed in striatum, was down-regulated by 50%

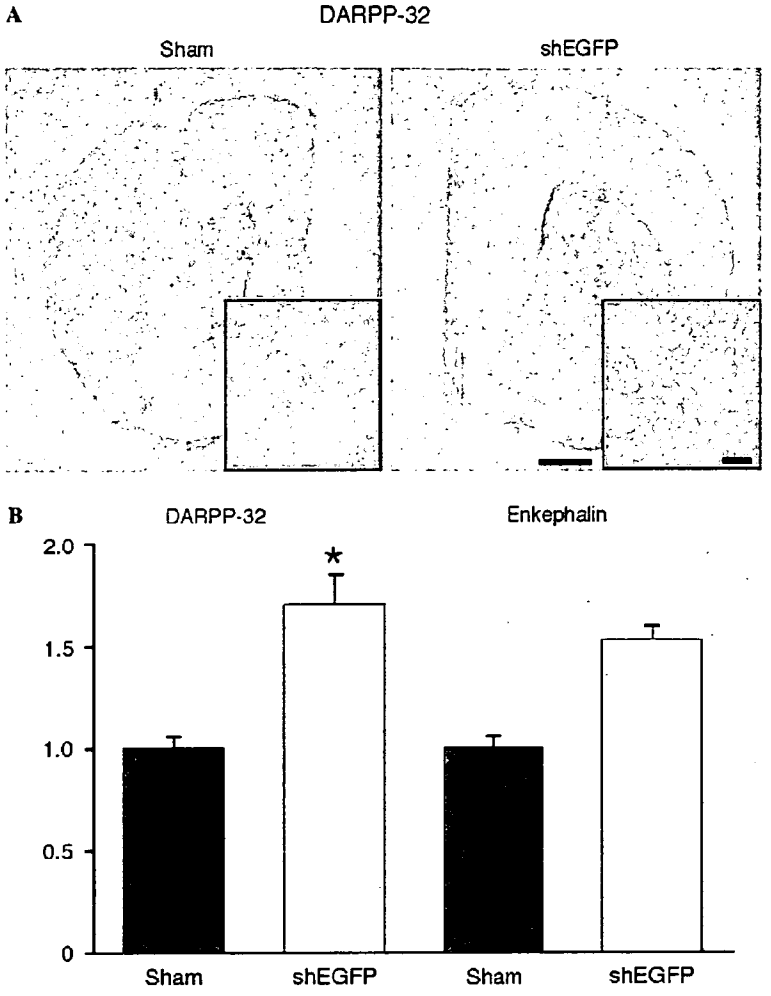

Fig. 4. shRNA restored DARPP-32 and enkephalin expression. (A) In situ hybridization of DARPP-32 at 24 weeks old after rAAV-shEGFP injection into the striatum at 9-week-old. Scale bar shows 1 mm. Higher magnification images of striatum are shown in inset, respectively, and scale bar is 20 μm. (B) DARPP-32 and enkephalin mRNA expression in striatum was determined by TaqMan RT-PCR analysis at 24 weeks after rAAV-shEGFP injection into the striatum performed at 12 weeks old. The expression levels of mRNA were normalized by that of GAPDH. DARPP-32 showed a significant increase in the shEGFP-injected side and enkephalin showed not significant but the tendency to restore. The values are given as means ± SEM ($n = 3$). $^{*}p < 0.05$.

in the 8-week-old HD190QG mouse compared with wild-type [21]. Here, we showed the restoration of DARPP-32 expression. Although the pathology was improved as shown in this report, we could not observe apparent improvement of the symptom or life span in this experiment. This is partly due to the injection was performed only in the one side to confirm the amelioration of the pathology and due to the injection time point, which restricted the full restoration of the function. Further study to determine the critical time of viral transduction for the functional recovery is necessary.

In this study, we used shRNA against EGFP for HD190QG mouse to suppress only the transgene. This shEGFP is designed to modulate mutant htt expression in our animal model but not applicable to the clinical investigation of human HD gene therapy. Although either siRNA or shRNA against htt was produced and investigated previously [17–19], this siRNA sequence reduced not only mutant htt but also wild-type htt simultaneously. Since wild-type htt is essential to embryogenesis, the complete loss of wild-type htt results in embryonic lethality and reduction of wild-type htt leads to behavioral abnormalities and neuronal loss [33]. In fact, loss of wild-type htt in YAC128 mice induced motor dysfunction and survival was worse compared with YAC128 mice expressing wild-type htt [33]. For these reasons, it is required to design a siRNA sequence, which selectively silences mutant htt but not wild-type htt. When a technology is developed to solve this issue, RNAi-based therapy would be practical for pre- and post-symptomatic treatment strategy for HD therapy [15,24].

In summary, we showed that RNAi dramatically improved HD-associated pathological abnormalities in a mouse model of HD, although the treatment was carried out after onset of symptom. Our data suggested that reduction of mutant gene expression by RNAi would be

promising to attenuate disease progression in post-symptomatic neurodegenerative disorders.

Acknowledgments

The authors thank Dr. John A. Chiorini for providing pAAV5-RNL and pAAV5-RepCap (identical to 5Rep-CapB) and Avigen, Inc. (Alameda, CA) for providing pAAV-LacZ, pHLP19, and pAdeno. We also thank Drs. Nobuhisa Iwata, Takaomi Saido, Mayumi Okada, and Ms. Miyoko Mitsu for their technical supports and Drs. Joanna Doumanis and Hong-Kit Wong for their critical readings. This work was supported in part by grants from Grants-in-Aid for Scientific Research on Priority Areas 17025044 from The Ministry of Education, Culture, Sports, Science and Technology (MEXT) and the Ministry of Health, Labour and Welfare.

References

[1] J.F. Gusella, M.E. MacDonald, Molecular genetics: unmasking polyglutamine triggers in neurodegenerative disease, Nat. Rev. Neurosci. 1 (2000) 109–115.
[2] A.W. Dunah, H. Jeong, A. Griffin, Y.M. Kim, D.G. Standaert, S.M. Hersch, M.M. Mouradian, A.B. Young, N. Tanese, D. Krainc, Sp1 and TAFII130 transcriptional activity disrupted in early Huntington's disease, Science 296 (2002) 2238–2243.
[3] C.J. Cummings, M.A. Mancini, B. Antalffy, D.B. DeFranco, H.T. Orr, H.Y. Zoghbi, Chaperone suppression of aggregation and altered subcellular proteasome localization imply protein misfolding in SCA1, Nat. Genet. 19 (1998) 148–154.
[4] N.R. Jana, M. Tanaka, G. Wang, N. Nukina, Polyglutamine length-dependent interaction of Hsp40 and Hsp70 family chaperones with truncated N-terminal huntingtin: their role in suppression of aggregation and cellular toxicity, Hum. Mol. Genet. 9 (2000) 2009–2018.
[5] U. Nagaoka, K. Kim, N.R. Jana, H. Doi, M. Maruyama, K. Mitsui, F. Oyama, N. Nukina, Increased expression of p62 in expanded polyglutamine-expressing cells and its association with polyglutamine inclusions, J. Neurochem. 91 (2004) 57–68.
[6] H. Doi, K. Mitsui, M. Kurosawa, Y. Machida, Y. Kuroiwa, N. Nukina, Identification of ubiquitin-interacting proteins in purified polyglutamine aggregates, FEBS Lett. 571 (2004) 171–176.
[7] N.F. Bence, R.M. Sampat, R.R. Kopito, Impairment of the ubiquitin-proteasome system by protein aggregation, Science 292 (2001) 1552–1555.
[8] A.V. Panov, C.A. Gutekunst, B.R. Leavitt, M.R. Hayden, J.R. Burke, W.J. Strittmatter, J.T. Greenamyre, Early mitochondrial calcium defects in Huntington's disease are a direct effect of polyglutamines, Nat. Neurosci. 5 (2002) 731–736.
[9] I. Sanchez, C. Mahlke, J. Yuan, Pivotal role of oligomerization in expanded polyglutamine neurodegenerative disorders, Nature 421 (2003) 373–379.
[10] M. Tanaka, Y. Machida, S. Niu, T. Ikeda, N.R. Jana, H. Doi, M. Kurosawa, M. Nekooki, N. Nukina, Trehalose alleviates polyglutamine-mediated pathology in a mouse model of Huntington disease, Nat. Med. 10 (2004) 148–154.
[11] S.M. Elbashir, J. Harborth, W. Lendeckel, A. Yalcin, K. Weber, T. Tuschl, Duplexes of 21-nucleotide RNAs mediate RNA interference in cultured mammalian cells, Nature 411 (2001) 494–498.
[12] J.Y. Yu, S.L. DeRuiter, D.L. Turner, RNA interference by expression of short-interfering RNAs and hairpin RNAs in mammalian cells, Proc. Natl. Acad. Sci. USA 99 (2002) 6047–6052.
[13] A.P. McCaffrey, M.A. Kay, A story of mice and men, Gene Ther. 9 (2002) 1563.
[14] H. Hasuwa, K. Kaseda, T. Einarsdottir, M. Okabe, Small interfering RNA and gene silencing in transgenic mice and rats, FEBS Lett. 532 (2002) 227–230.
[15] G.S. Ralph, P.A. Radcliffe, D.M. Day, J.M. Carthy, M.A. Leroux, D.C. Lee, L.F. Wong, L.G. Bilsland, L. Greensmith, S.M. Kingsman, K.A. Mitrophanous, N.D. Mazarakis, M. Azzouz, Silencing mutant SOD1 using RNAi protects against neurodegeneration and extends survival in an ALS model, Nat. Med. 11 (2005) 429–433.
[16] H. Xia, Q. Mao, S.L. Eliason, S.Q. Harper, I.H. Martins, H.T. Orr, H.L. Paulson, L. Yang, R.M. Kotin, B.L. Davidson, RNAi suppresses polyglutamine-induced neurodegeneration in a model of spinocerebellar ataxia, Nat. Med. 10 (2004) 816–820.
[17] S.Q. Harper, P.D. Staber, X. He, S.L. Eliason, I.H. Martins, Q. Mao, L. Yang, R.M. Kotin, H.L. Paulson, B.L. Davidson, RNA interference improves motor and neuropathological abnormalities in a Huntington's disease mouse model, Proc. Natl. Acad. Sci. USA 102 (2005) 5820–5825.
[18] E. Rodriguez-Lebron, E.M. Denovan-Wright, K. Nash, A.S. Lewin, R.J. Mandel, Intrastriatal rAAV-mediated delivery of anti-huntingtin shRNAs induces partial reversal of disease progression in R6/1 Huntington's disease transgenic mice, Mol. Ther. 12 (2005) 618–633.
[19] Y.L. Wang, W. Liu, E. Wada, M. Murata, K. Wada, I. Kanazawa, Clinico-pathological rescue of a model mouse of Huntington's disease by siRNA, Neurosci. Res. (2005).
[20] A. Yamamoto, J.J. Lucas, R. Hen, Reversal of neuropathology and motor dysfunction in a conditional model of Huntington's disease, Cell 101 (2000) 57–66.
[21] S. Kotliarova, N.R. Jana, N. Sakamoto, M. Kurosawa, H. Miyazaki, M. Nekooki, H. Doi, Y. Machida, H.K. Wong, T. Suzuki, C. Uchikawa, Y. Kotliarov, K. Uchida, Y. Nagao, U. Nagaoka, A. Tamaoka, K. Oyanagi, F. Oyama, N. Nukina, Decreased expression of hypothalamic neuropeptides in Huntington disease transgenic mice with expanded polyglutamine-EGFP fluorescent aggregates, J. Neurochem. 93 (2005) 641–653.
[22] R.E. Campbell, O. Tour, A.E. Palmer, P.A. Steinbach, G.S. Baird, D.A. Zacharias, R.Y. Tsien, A monomeric red fluorescent protein, Proc. Natl. Acad. Sci. USA 99 (2002) 7877–7882.
[23] T. Okada, K. Shimazaki, T. Nomoto, T. Matsushita, H. Mizukami, M. Urabe, Y. Hanazono, A. Kume, K. Tobita, K. Ozawa, N. Kawai, Adeno-associated viral vector-mediated gene therapy of ischemia-induced neuronal death, Methods Enzymol. 346 (2002) 378–393.
[24] T. Okada, T. Nomoto, T. Yoshioka, M. Nonaka-Sarukawa, T. Ito, T. Ogura, M. Iwata-Okada, R. Uchibori, K. Shimazaki, H. Mizukami, A. Kume, K. Ozawa, Large-scale production of recombinant viruses by use of a large culture vessel with active gassing, Hum. Gene Ther. 16 (2005) 1212–1218.
[25] S.W. Davies, M. Turmaine, B.A. Cozens, M. DiFiglia, A.H. Sharp, C.A. Ross, E. Scherzinger, E.E. Wanker, L. Mangiarini, G.P. Bates, Formation of neuronal intranuclear inclusions underlies the neurological dysfunction in mice transgenic for the HD mutation, Cell 90 (1997) 537–548.
[26] R. Luthi-Carter, A. Strand, N.L. Peters, S.M. Solano, Z.R. Hollingsworth, A.S. Menon, A.S. Frey, B.S. Spektor, E.B. Penney, G. Schilling, C.A. Ross, D.R. Borchelt, S.J. Tapscott, A.B. Young, J.H. Cha, J.M. Olson, Decreased expression of striatal signaling genes in a mouse model of Huntington's disease, Hum. Mol. Genet. 9 (2000) 1259–1271.
[27] R.J. Ferrante, J.K. Kubilus, J. Lee, H. Ryu, A. Beesen, B. Zucker, K. Smith, N.W. Kowall, R.R. Ratan, R. Luthi-Carter, S.M. Hersch, Histone deacetylase inhibition by sodium butyrate chemotherapy ameliorates the neurodegenerative phenotype in Huntington's disease mice, J. Neurosci. 23 (2003) 9418–9427.
[28] R.J. Ferrante, O.A. Andreassen, B.G. Jenkins, A. Dedeoglu, S. Kuemmerle, J.K. Kubilus, R. Kaddurah-Daouk, S.M. Hersch, M.F.

Beal, Neuroprotective effects of creatine in a transgenic mouse model of Huntington's disease, J. Neurosci. 20 (2000) 4389–4397.

[29] M. Chen, V.O. Ona, M. Li, R.J. Ferrante, K.B. Fink, S. Zhu, J. Bian, L. Guo, L.A. Farrell, S.M. Hersch, W. Hobbs, J.P. Vonsattel, J.H. Cha, R.M. Friedlander, Minocycline inhibits caspase-1 and caspase-3 expression and delays mortality in a transgenic mouse model of Huntington disease, Nat. Med. 6 (2000) 797–801.

[30] M.V. Karpuj, M.W. Becher, J.E. Springer, D. Chabas, S. Youssef, R. Pedotti, D. Mitchell, L. Steinman, Prolonged survival and decreased abnormal movements in transgenic model of Huntington disease, with administration of the transglutaminase inhibitor cystamine, Nat. Med. 8 (2002) 143–149.

[31] C. Burger, O.S. Gorbatyuk, M.J. Velardo, C.S. Peden, P. Williams, S. Zolotukhin, P.J. Reier, R.J. Mandel, N. Muzyczka, Recombinant AAV viral vectors pseudotyped with viral capsids from serotypes 1, 2, 5 display differential efficiency and cell tropism after delivery to different regions of the central nervous system, Mol. Ther. 10 (2004) 302–317.

[32] M.Y. Mastakov, K. Baer, R.M. Kotin, M.J. During, Recombinant adeno-associated virus serotypes 2- and 5-mediated gene transfer in the mammalian brain: quantitative analysis of heparin co-infusion, Mol. Ther. 5 (2002) 371–380.

[33] J.M. Van Raamsdonk, J. Pearson, D.A. Rogers, N. Bissada, A.W. Vogl, M.R. Hayden, B.R. Leavitt, Loss of wild-type huntingtin influences motor dysfunction and survival in the YAC128 mouse model of Huntington disease, Hum. Mol. Genet. 14 (2005) 1379–1392.

ARTICLE

doi:10.1016/j.ymthe.2005.11.010

A Histone Deacetylase Inhibitor Enhances Recombinant Adeno-associated Virus-Mediated Gene Expression in Tumor Cells

Takashi Okada,[1,*] Ryosuke Uchibori,[1] Mayumi Iwata-Okada,[2] Masafumi Takahashi,[3] Tatsuya Nomoto,[1] Mutsuko Nonaka-Sarukawa,[1] Takayuki Ito,[1] Yuhe Liu,[1] Hiroaki Mizukami,[1] Akihiro Kume,[1] Eiji Kobayashi,[3] and Keiya Ozawa[1,2]

[1]*Division of Genetic Therapeutics,* [3]*Division of Organ Replacement Research, Center for Molecular Medicine, and* [2]*Division of Hematology, Department of Medicine, Jichi Medical School, Tochigi 329-0498, Japan*

**To whom correspondence and reprint requests should be addressed at the Division of Genetic Therapeutics, Center for Molecular Medicine, Jichi Medical School, 3311-1 Yakushiji, Minami-Kawachi, Tochigi 329-0498, Japan. Fax: +81 285 44 8675. E-mail: tokada@jichi.ac.jp.*

Available online 4 January 2006

The transduction of cancer cells using recombinant adeno-associated virus (rAAV) occurs with low efficiency, which limits its utility in cancer gene therapy. We have previously sought to enhance rAAV-mediated transduction of cancer cells by applying DNA-damaging stresses. In this study, we examined the effects of the histone deacetylase inhibitor FR901228 on tumor transduction mediated by rAAV types 2 and 5. FR901228 treatment significantly improved the expression of the transgene in four cancer cell lines. The cell surface levels of alpha v integrin, FGF-R1, and PDGF-R were modestly enhanced by the presence of FR901228. These results suggest that the superior transduction induced by the HDAC inhibitor was due to an enhancement of transgene expression rather than increased viral entry. Furthermore, we characterized the association of the acetylated histone H3 in the episomal AAV vector genome by using the chromatin immunoprecipitation assay. The results suggest that the superior transduction may be related to the proposed histone-associated chromatin form of the rAAV concatemer in transduced cells. In the analysis with subcutaneous tumor models, strong enhancement of the transgene expression as well as therapeutic effect was confirmed *in vivo*. The use of this HDAC inhibitor may enhance the utility of rAAV-mediated transduction strategies for cancer gene therapy.

Key Words: histone deacetylase inhibitor, AAV vector, cancer

INTRODUCTION

Recombinant adeno-associated virus (rAAV) has been of considerable interest to developers of clinical gene therapies [1,2]. This is because, unlike adenoviruses, the introduction of AAV vectors has not been associated with significant inflammation either experimentally or clinically [3]. Furthermore, diseases associated with AAV have not been found in human or animal populations. However, the transduction of cancer cells using rAAV occurs with very low efficiency, which limits its utility in gene therapy. Consequently, we have sought to enhance rAAV-mediated transduction of cancer cells by applying DNA-damaging stresses such as γ-rays or anticancer agents [4–6].

An alternative approach to improving the rAAV-mediated transduction of tumor cells may be to enhance transcription in the target cells. One technique to bring about this event may be to apply a histone deacetylase (HDAC) inhibitor, since HDAC inhibitors are known to regulate the transcription of various genes. Significantly, an HDAC inhibitor increases adenovirus-mediated transduction of cancer cell lines because it enhances the levels of the viral receptor on the cell surface [7]. On the other hand, the effects of HDAC inhibitors on rAAV-mediated transduction of tumor cells have not yet been fully elucidated. Treatment with an HDAC inhibitor causes gene expression from a silenced rAAV genome that has been integrated into the host's genome to recover [8]. However, rAAV exists mostly as an extrachromosomal genome rather than as an integrated genome, and this extrachromosomal form is the primary source of rAAV-mediated gene expression [9]. Therefore, the HDAC inhibitor-mediated recovery of expression from the integrated and silenced genome does not reflect a typical situation of rAAV-mediated transduction. Whereas no

1525-0016/$30.00

clear mechanism has been determined for the effect on the episomal vector-mediated expression, the histone deacetylase inhibitor should also contribute to the enhanced transcription before integration occurs.

Here we show that HDAC inhibitors markedly enhance the transgene expression immediately after rAAV-mediated transduction of tumor cells *in vitro* as well as *in vivo*. Our data also suggest that the vector genome in the cells is in the histone-associated chromatin form, which is capable of superior transcription. HDAC inhibitors may improve tumor cell transduction by enhancing the acetylation of the histone-associated chromatin of the rAAV genome.

RESULTS

Effects of FR901228 Treatment on the Transduction of U251MG Cells with rAAV

To analyze whether an HDAC inhibitor can also improve rAAV-mediated gene expression soon after the infection,

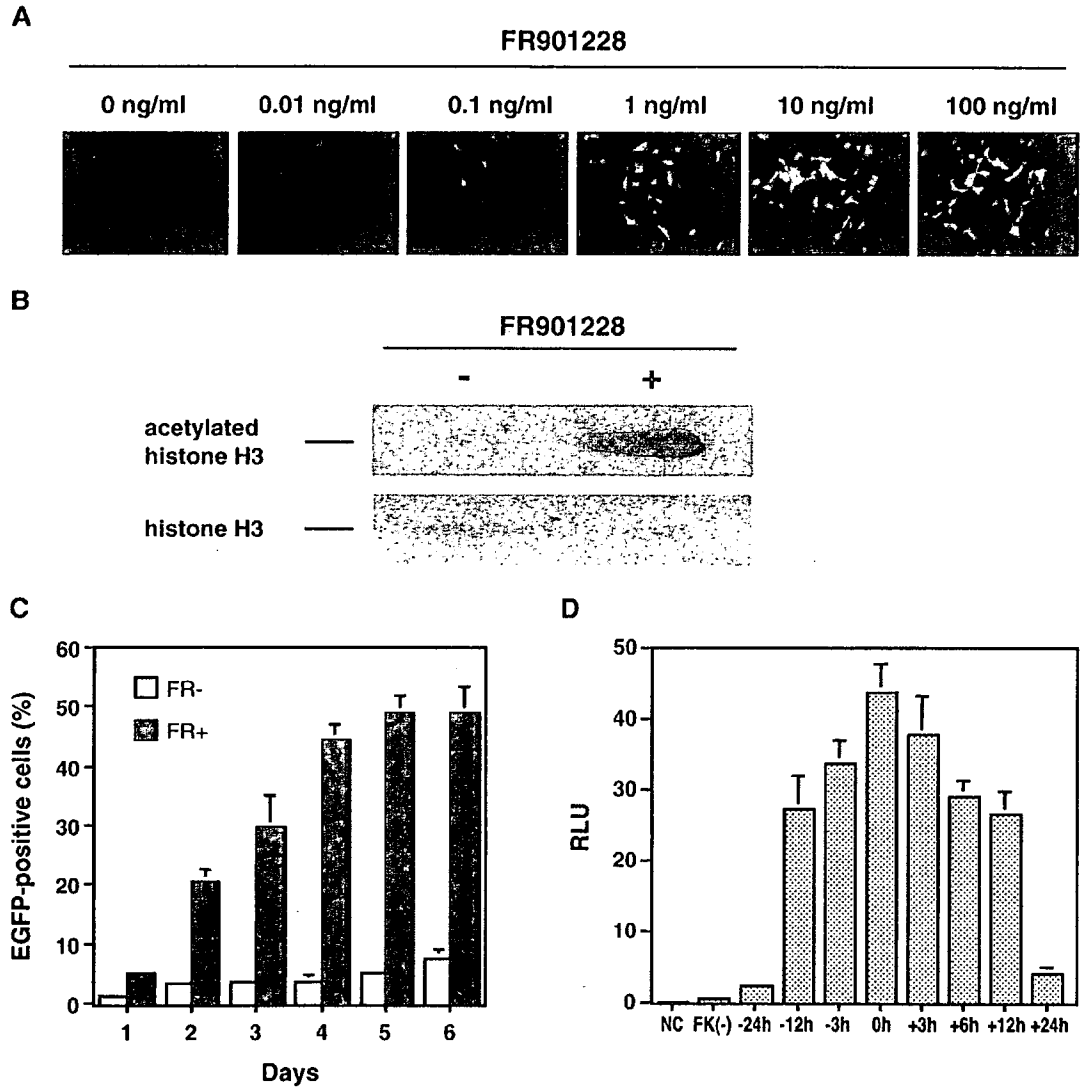

FIG. 1. (A) Effects of FR901228 treatment on the transduction of U251MG cells with rAAV. U251MG cells were infected with 1×10^4 genome copies/cell of AAV2EGFP in the presence of various concentrations of FR901228. EGFP expression was observed 24 h after infection. (B) Detection of the histone acetylation in U251MG cells caused by FR901228 treatment. Cells were incubated in the presence or absence of FR901228 for 24 h. The levels of acetylated histone H3 and histone H3 were determined by Western blot analysis. Histone H3 serves as a loading control. (C) The percentage of EGFP-positive cells at various time points after transduction with AAV2EGFP in the presence (FR+) or absence (FR−) of 1 ng/ml FR901228 was determined by FACS. Cells were infected with AAV2EGFP at 1×10^3 genome copies/cell. The data shown are the means and standard deviations of three independent experiments. (D) The kinetics of the effect on the FR901228-assisted transduction of U251MG cells. Cells were treated with FR901228 at various time points around the transduction with rAAV expressing luciferase as indicated. Luciferase assay was performed on the luminometer 48 h after the transduction.

doi:10.1016/j.ymthe.2005.11.010

we transduced U-251MG human glioma cells with EGFP-expressing rAAV (AAV2EGFP) in the presence of the HDAC inhibitor FR901228. We found that FR901228 treatment improved the AAV2EGFP-mediated gene expression in a dose-dependent manner early after the infection (Fig. 1A). The fact that FR901228 also enhanced the acetylation of the histones in the cells was confirmed by Western blot analysis (Fig. 1B). To assess when gene expression was maximal, we transduced U251MG cells with AAV2EGFP in the presence or absence of 1 ng/ml FR901228 and assessed EGFP expression at various time points after transduction (Fig. 1C). This revealed that the enhancement of gene expression depended on the incubation period and required 4 days before the expression reach a plateau. To analyze the kinetics of the effect on the FR901228-assisted transduction of U251MG cells, cells were treated with FR901228 at various time points around the transduction with luciferase-expressing rAAV type 2 (AAV2-Luc) (Fig. 1D). As a result, the transduction efficiency peaked when cells were treated with FR901228 at the time of virus transduction.

TABLE 1: Relative expression of FGF-R1 and PDGF-R in U251MG cells treated with recombinant AAV alone (1×10^4 genome copies/cell) or together with FR901228 (0.3 or 3 ng/ml) for 24 h as analyzed by quantitative PCR

	$2^{\text{correctedΔCt (GAPDH - target)}}$	
FR901228 (ng/ml)	FGF-R1	PDGF-Rα
0	1.00	1.00
0.3	1.28	1.77
3	1.60	2.30

The relative expression of the target mRNA was determined as the ratio of the expression in U251MG cells treated with recombinant AAV and FR901228 to that in U251MG cells treated with recombinant AAV alone. Data are means ($n = 5$).

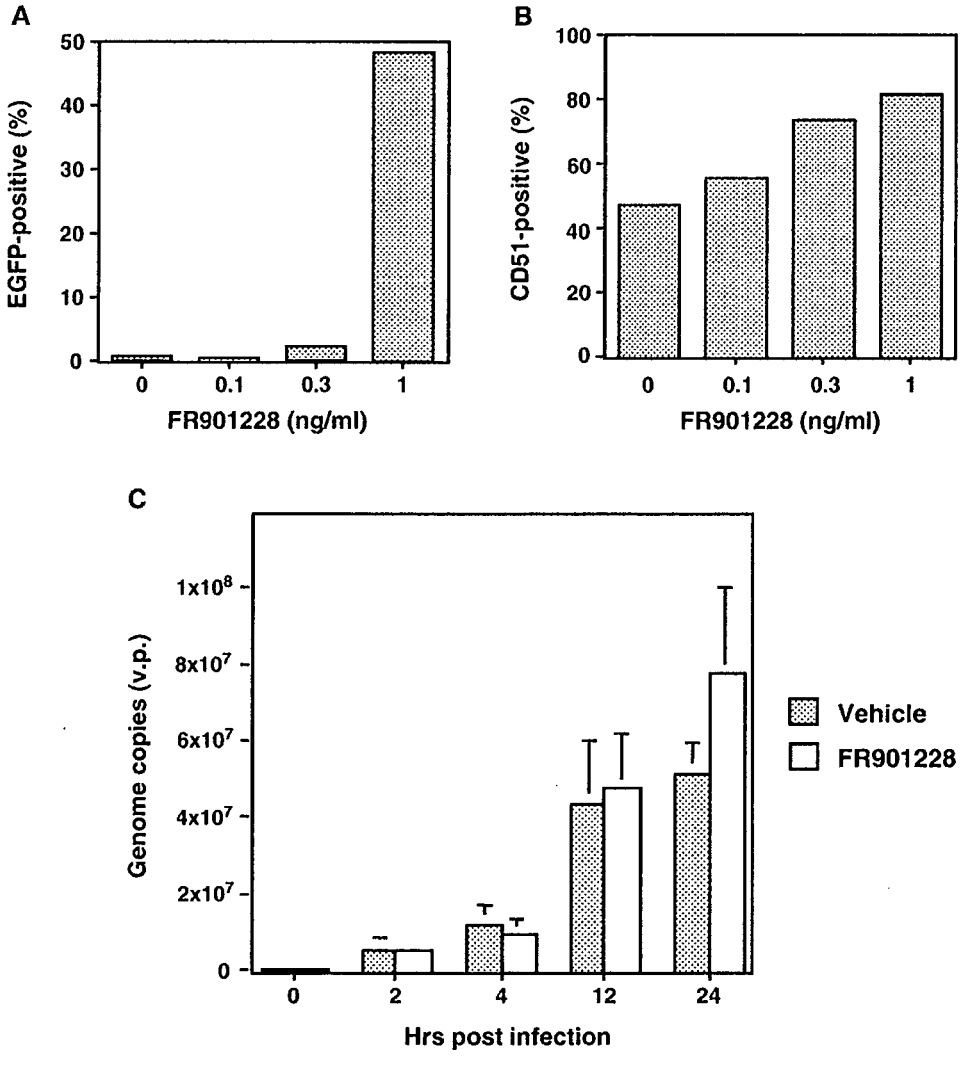

FIG. 2. (A) Percentage of EGFP-positive U251MG cells after transduction with 1×10^4 genome copies/cell of AAV2EGFP in the presence of various concentrations of FR901228. The cells were analyzed 24 h after the transduction for EGFP expression by FACS. The data shown are the average percentages of EGFP-positive cells after three independent transductions. (B) Integrin expression in transduced cells is only modestly enhanced by FR901228 treatment. The cells were stained 24 h after the transduction with monoclonal antibodies to CD51 (integrin v chain, clone 13C2) and analyzed by FACS. The data shown are the average percentages of positive cells after three independent transductions. (C) Transgene copy number in U251MG cells transduced with 1×10^4 genome copies/cell of AAV2EGFP in the presence of 1 ng/ml FR901228. The copy number of the transgene was estimated by real-time PCR at 0, 2, 4, 12, and 24 h after the rAAV infection.

Effects on Receptor Expression and Viral Entry

To determine if FR901228 acted by enhancing the entry of rAAV, we infected U251MG cells with AAV2EGFP in the presence of various concentrations of FR901228 and then analyzed the EGFP and alpha v integrin levels in the cells by fluorescence-activated cell sorting (FACS). This analysis showed that 24 h after AAV2EGFP infection with 1 ng/ml FR901228, 48% of the U251MG cells were EGFP-positive, whereas at lower concentrations of FR901228 only very few cells were EGFP-positive (Fig. 2A). However, this FR901228 concentration range (0.3–1 ng/ml) only modestly enhanced the levels of AAV2 coreceptor, alpha v integrin (Fig. 2B). In addition, when we estimated the amount of the rAAV genome in the transduced cells by real-time quantitative PCR analysis, we found that FR901228 treatment did not significantly affect the copy number of the rAAV (Fig. 2C). Furthermore, we also estimated the effect of FR901228 on the expression of coreceptors for the AAV. FR901228 moderately

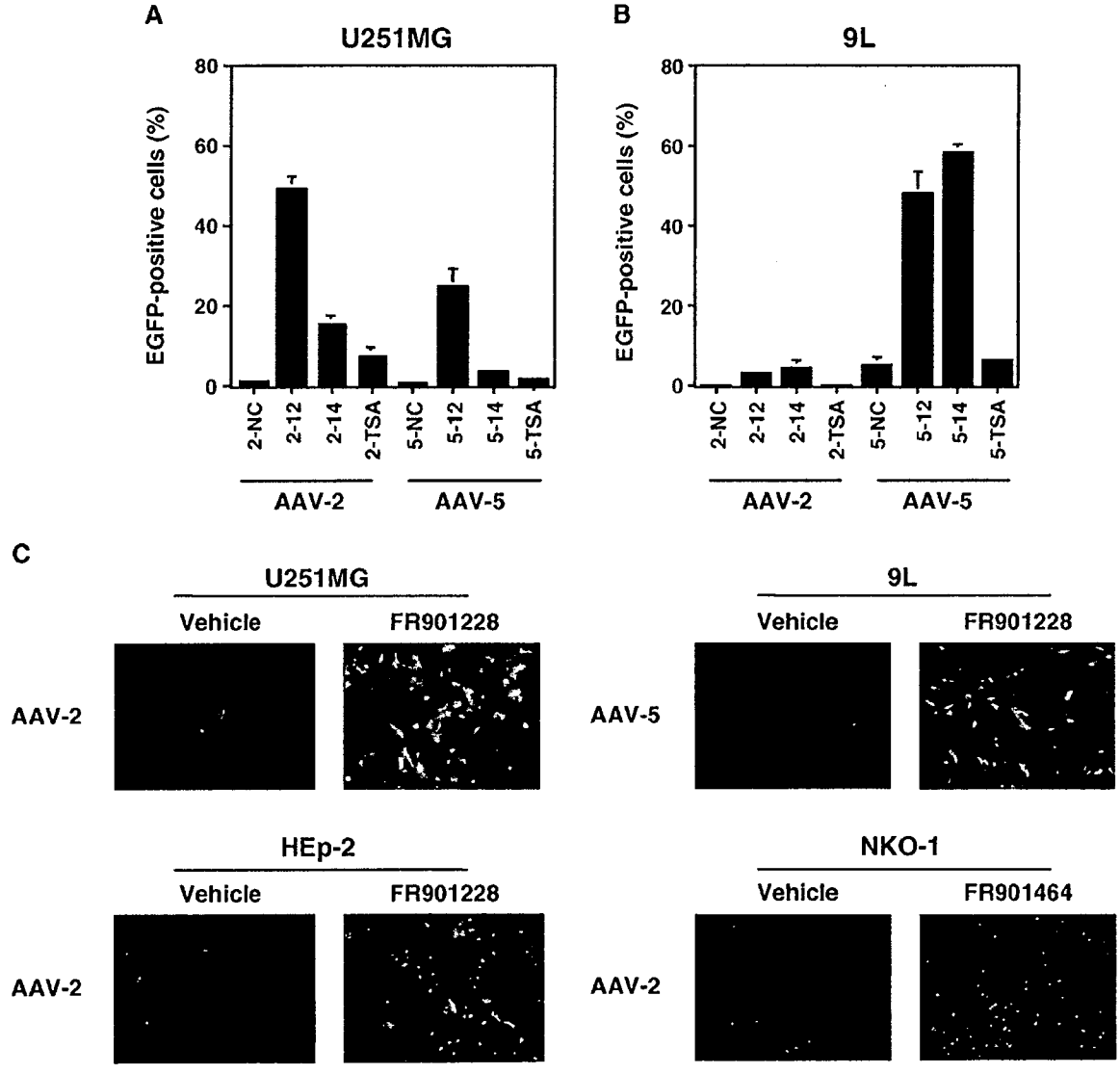

FIG. 3. (A, B) EGFP expression by AAV2EGFP and AAV5EGFP differs depending on the tumor cell being transduced. U251MG or 9L cells were infected with 1 × 10^4 genome copies/cell of AAV2EGFP (2) or AAV5EGFP (5) in the presence of vehicle (NC) or 1 ng/ml of various HDAC inhibitors, FR901228 (12), FR901464 (14), or TSA. The cells were analyzed by FACS 24 h after the infection. The data show the average percentages of EGFP-positive cells after three independent transductions + SD. (C) Representative data of the enhanced transgene expression by HDAC inhibitors in various cell lines infected with AAV vectors. Twenty-four hours after the AAV2EGFP or AAV5EGFP infection at 1 × 10^4 genome copies/cell with 1 ng/ml of the FR901228 or FR901464, cells were examined under the fluorescence microscope.

doi:10.1016/j.ymthe.2005.11.010

increased mRNA levels of fibroblast growth factor receptor 1 (FGF-R1) and platelet-derived growth factor receptor (PDGF-R), although the augmentation was not enough to explain the drastic increase of the expression (Table 1).

Transduction of Tumor Cells with AAV Vectors Derived from Distinct Serotypes

Type 2 and type 5 rAAV differed from each other in the efficiency of their transduction of U251MG and the 9L glioma cells. Although FR901228 and other HDAC inhibitors (FR901464 or trichostatin A (TSA)) remarkably enhanced the transduction of both rAAVs in general, AAV2EGFP-mediated transduction of U251MG cells was more efficient than AAV5EGFP-mediated transduction while AAV5EGFP-mediated transduction of 9L cells was better than AAV2EGFP-mediated transduction (Figs. 3A and 3B). FR901228 and FR901464 also had promoting effects on AAV2EGFP- and AAV5EGFP-mediated transduction of the head and neck cancer cell lines HEp-2 and NKO-1 (Fig. 3C).

Chromatin Modification with FR901228

We characterized chromatin composition of the episomal AAV vector genome by using the chromatin immunoprecipitation (ChIP) assay. ChIP is a technique to test for the presence of certain DNA-binding proteins that might modulate chromatin structure and/or transcriptional characteristics of the specific region of DNA with which they are associated. We made use of polyclonal antibodies generated against histone H3 as well as acetylated histone H3, which have been linked to chromatin modification and regulation of transcription. The primers for the CMV promoter region in the AAV vector genome gave a higher level of PCR product when used on templates from FR901228-treated cells compared to those from cells without FR901228 treatment. Higher levels of acetylated histone H3 were found on the CMV promoter region of the AAV vector versus the GAPDH promoter region of the cellular DNA (Table 2A). In contrast, enrichment of acetylated histone H3-associated DNA was not significant on plasmid vector genome irrespective of the presence of the ITR (Table 2B).

FR901228-Assisted Enhancement of Tumor Transduction *in Vivo*

In the analysis using optical bioluminescence imaging of the subcutaneous tumors, we confirmed drastic enhancement of the luciferase gene expression *in vivo* (Fig. 4A). The signal intensity in animals treated with FR901228 (n = 5, [1.5 ± 0.9] × 10^6 photons/s/cm^2/sr) was 37.4-fold higher than in control animals (n = 3, [4.0 ± 2.4] × 10^4 photons/s/cm^2/sr). A subcutaneous

TABLE 2: PCR amplification of immunoprecipitated DNA

(A) Chromatin composition of episomal AAV vector genome was characterized by using the chromatin immunoprecipitation assay

Ab of interest	FR901228	$2^{\text{correctedΔCt (GAPDHprom – CMVprom)}}$
Rabbit IgG	–	<0.001
Rabbit IgG	+	<0.001
Anti-histone H3	–	1.0 ± 1.8
Anti-histone H3	+	7.3 ± 1.4
Anti-acetyl histone H3	–	1.0 ± 0.4] < 0.0001
Anti-acetyl histone H3	+	22.0 ± 0.8]

(B) Cells were transfected with a plasmid harboring the EGFP expression cassette under the CMV promoter (pEGFP) or a plasmid carrying an identical EGFP expression cassette flanked by ITR regions (pITR-EGFP)

Plasmid	Ab of interest	FR901228	$2^{\text{correctedΔCt (GAPDHprom – CMVprom)}}$
pEGFP	Rabbit IgG	–	<0.001
	Rabbit IgG	+	<0.001
	Anti-acetyl histone H3	–	1.0
	Anti-acetyl histone H3	+	1.3
pITR-EGFP	Rabbit IgG	–	<0.001
	Rabbit IgG	+	<0.001
	Anti-acetyl histone H3	–	1.0
	Anti-acetyl histone H3	+	1.2

U251MG cells were transduced with AAV vector at 1 × 10^4 genome copies/cell in the presence or absence of 1 ng/ml FR901228. Twenty-four hours after the transduction, chromatin proteins of interest were cross-linked to DNA by formaldehyde. Shared DNA was immunoprecipitated with histone H3 antibody or acetylated histone H3 antibody to enrich for the CMV promoter region or GAPDH promoter region. Relative differences in the levels of immunoprecipitated DNA, which are reflective of the levels of the chromatin protein of interest occupying a particular island, between different promoter regions and cell treatment with FR901228 were quantified by quantitative PCR.

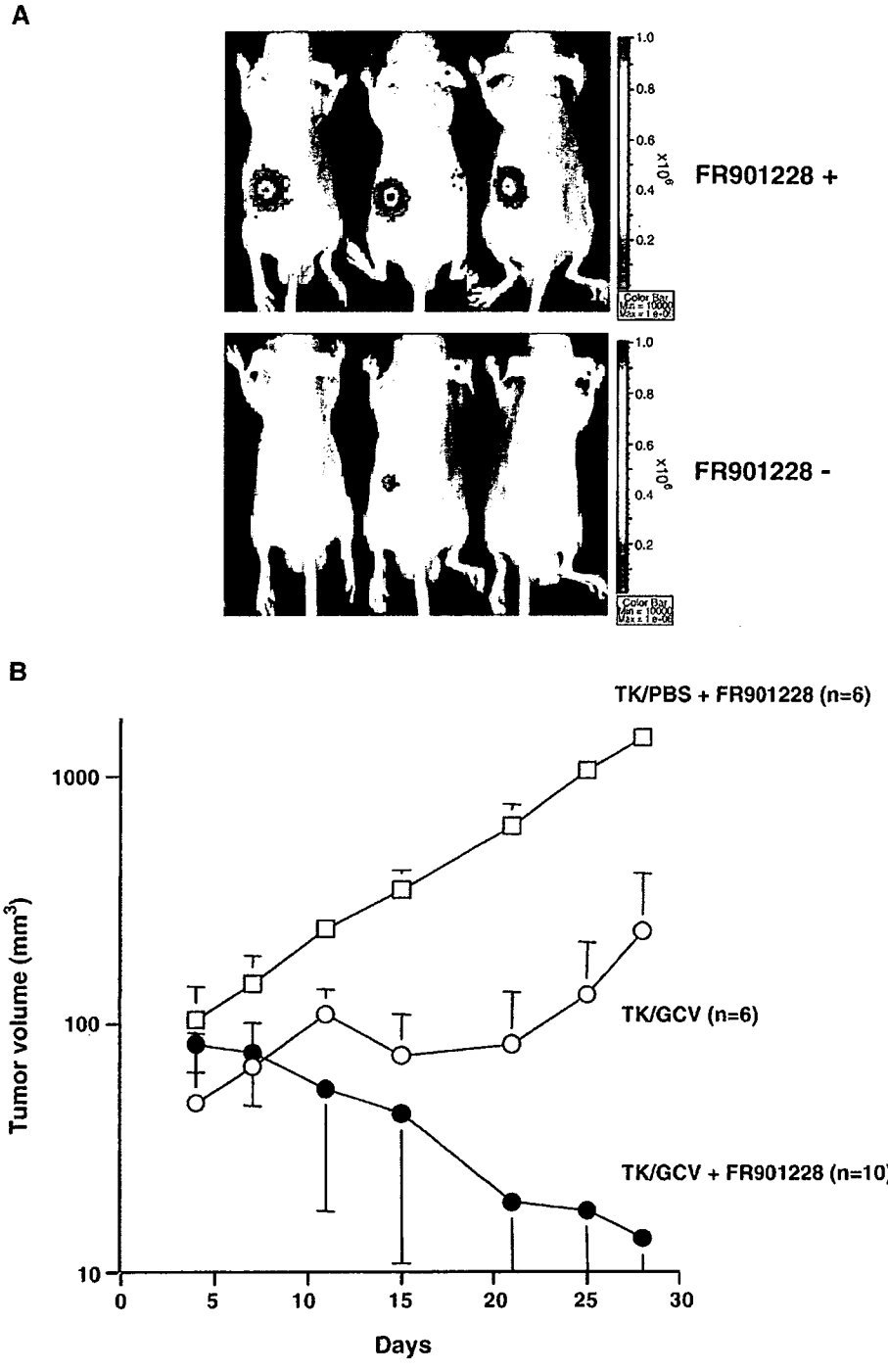

FIG. 4. (A) FR901228-assisted enhancement of tumor transduction *in vivo*. U251MG cells were mixed with PBS (FR901228–, $n = 3$) or transduced with a recombinant AAV2 expressing luciferase (AAV2Luc) at 1×10^4 genome copies/cell for 1 h (FR901228+, $n = 5$), and then 3×10^6 of the transduced cells in 100 μl PBS were inoculated subcutaneously into the BALB/c mice along with the intraperitoneal injection of FR901228 at 1 mg/kg. Twenty-four hours after administration of the FR901228, optical bioluminescence imaging was performed using the CCD camera. (B) The effects of FR901228 on the rAAV-mediated transduction for 9L tumor elimination *in vivo*. Cells were transduced with AAV5TK at 1×10^4 genome copies/cell for 1 h, and then 3×10^6 of the transduced cells in 100 μl PBS containing 25% (v/v) basement membrane matrix were inoculated subcutaneously into the BALB/c mice. The tumor-bearing animals received intraperitoneal injection of FR901228 at 3 mg/kg (group 1, $n = 6$; group 3, $n = 10$) or PBS (group 2, $n = 6$). The animals were also exposed to ganciclovir (GCV) at 100 mg/kg per day (groups 2 and 3) or PBS (group 1) for 14 consecutive days by intraperitoneal placement of the miniosmotic pumps.

tumor model with athymic nude mice demonstrated that the combination of AAV-mediated transduction for HSV-*tk*/GCV therapy and FR901228 treatment ($n = 10$) resulted in statistically significant reduction of tumor growth relative to HSV-*tk*/GCV therapy without FR901228 treatment (unpaired t test, $P < 0.05$, $n = 6$; Fig. 4B). When the tumor-bearing animals were treated with GCV and FR901228, 8 of 10 tumors were eliminated at 4 weeks after transduction.

Discussion

HDAC inhibitors significantly improved the expression of the transgene in cancer cells. The enhancement of the coreceptor level was modest and copy number of the

doi:10.1016/j.ymthe.2005.11.010

rAAV in the transduced cells was also modestly affected by the FR901228 treatment. Furthermore, association of the acetylated histone H3 in the episomal AAV vector genome was demonstrated by using the chromatin immunoprecipitation assay. In the analysis with the subcutaneous tumor models, strong enhancement of the transgene expression as well as therapeutic effect was confirmed *in vivo*.

Treatment with an HDAC inhibitor is known to cause the recovery of the gene expression of a rAAV vector genome that has been integrated and silenced after long-term selection [8]. However, rAAV occurs mostly as extrachromosomal genomes rather than as integrated genomes, and these extrachromosomal forms are the primary source of rAAV-mediated gene expression early after transduction [9]. There has been no direct investigation of the effects of HDAC inhibitors on the rAAV-mediated transient gene expression. We examined whether the HDAC inhibitor could contribute to the enhanced transcription before integration occurs.

FR901228 treatment significantly improved the transient expression of the transgene in four cancer cell lines. The FR901228 treatment improved the rAAV-mediated gene transfer in a dose-dependent manner, and the highest enhancement was observed in the U251MG cells with AAV2EGFP. In the U251MG cells, the cell surface levels of alpha v integrin, FGF-R1, and PDGF-R were only modestly enhanced by the presence of FR901228. These observations contrast with a previous report that suggested that FR901228 enhanced adenovirus transduction by increasing CAR and v integrin RNA levels, thereby enhancing viral entry [7]. However, their study did not demonstrate that these increased RNA levels were associated with increased protein levels or kinetics. In our study, a kinetic analysis of the effect on the FR901228-assisted AAV-mediated transduction of U251MG cells showed that the transduction efficiency peaked when cells were treated with FR901228 at the time of transduction. This is in sharp contrast to the case of the effect of FR901228 on the enhanced adenovirus-mediated transduction. Since enhanced viral entry into the cell is a primary function of FR901228 regarding improved adenovirus transduction, transduction efficiency of the adenovirus was preferentially enhanced when the cells were pretreated with FR901228 before transduction [10].

Interestingly, we observed that type 2 and type 5 rAAV differed from each other in the efficiency of their transduction of the U251MG and 9L cells. The differences in the transduction efficiency of the AAV vectors derived from distinct serotypes may be due to the fact that each AAV serotype recognizes a different receptor and that different cell types may express different levels of these receptors. Type 2 AAV uses the cell surface heparan sulfate proteoglycan (HSPG) as a receptor [11]. However, cell surface expression of HSPG alone is insufficient for type 2 AAV infection and FGF-R1 is also required as a coreceptor for successful viral entry into the host cell [12]. Type 5 AAV transduction requires 2,3-linked sialic acid [13] as well as PDGF-R [14] for efficient binding and transduction. These observations indicate that optimized expression of a transgene borne by rAAV will require the careful selection of the appropriate vector serotype with respect to the target cell.

Our data also suggest that the use of FR901228 in combination with AAV vector infection may improve viral entry into the cells, but also requires additional mechanisms to benefit the target cells for the efficient transduction. Association of the acetylated histone H3 in the episomal AAV vector genome was characterized by using the chromatin immunoprecipitation assay. Characterization of the chromatin modification in the rAAV genome with FR901228 suggested that improved expression of the transgene depends on the chromatin state of the AAV genome in the infected cells rather than viral entry. These results suggest that the superior transduction induced by HDAC inhibitor treatment is actually due to an enhancement of transgene expression associated with chromatin modification rather than to increased viral entry. Thus, epigenetic regulatory mechanisms may be involved in the HDAC inhibitor-mediated improvement of the transduction of cancer cells with rAAV. The rAAV concatemer may need to be present in a histone-associated chromatin form in the cells before efficient transgene expression can occur.

Our study suggests that the improved rAAV-mediated transduction induced by HDAC inhibitor was due to an enhancement of transgene expression rather than increased viral entry. This phenomenon may be related to the proposed histone-associated chromatin form of the rAAV concatemer in transduced cells. The depsipeptide fermentation product FR901228 is currently being tested in clinical trials as an anti-cancer drug. Therefore, to utilize such a compound to assist rAAV-mediated cancer gene therapy is theoretically and practically reasonable. The use of HDAC inhibitors may enhance the utility of rAAV-mediated transduction strategies for future clinical investigation.

Materials and Methods

Recombinant AAV production. The EGFP expression cassette driven by the CMV promoter was ligated into pAAVLacZ [15] and pAAV5-RNL [16] to form the proviral plasmids pAAV2EGFP and pAAV5EGFP. rAAV types 2 and 5 that express the EGFP gene (AAV2EGFP and AAV5EGFP) were generated using the proviral plasmids. The luciferase expression cassette driven by the CMV promoter in pLNCL [17] was cloned into pAAVLacZ to create pAAV2Luc. A rAAV type 2 that expresses the luciferase gene (AAV2Luc) was generated using pAAV2Luc. Likewise, the HSV-*tk* cDNA contained in the pAVS6TK [18] was subcloned into pAAV5-RNL to create pAAV5TK. A rAAV type 5 that expresses the HSV-*tk* gene driven by the CMV promoter (AAV5TK) was generated using pAAV5TK. Transfection of 293 cells with the proviral plasmid, AAV helper plasmid pAAV2H [15] or pAAV5H [16], and adenoviral helper plasmid pAdeno was performed according to the previously described protocol [19] associated with an